Subcooled Pool Boiling CHF in Ethanol

Jongdoc PARK * Katsuya FUKUDA** and Qiusheng LIU**

Abstract

Steady-state and transient critical heat fluxes (CHFs) were measured using a 1.0 mm diameter horizontal cylinder in a pool of highly wetting liquid, such as ethanol, due to steady and transient heat generation rate for wide range of subcoolings and pressures. Boiling CHF was assumed to happen based on a kind of hydrodynamic instability (HI) at CHF, and the model is supposed that the increase in vapor generation from the cylinder surface causes a limit of the steady-state vapor escape flow when CHF occurs. However, it has been understood that the CHF value changes systematically depending on experimental conditions according to a series of experiment. As the reason, a large part of the transition processes to film boiling at CHF highly subcooled liquid at high pressure was not explained by the mechanism of heat transfer crisis based on the HI model. Another mechanism assumed is that the transition occurs due to the explosive-like heterogeneous spontaneous nucleation (HSN) in originally flooded cavities on the cylinder surface in liquid. This research is to find the mechanism in the transition boiling CHF, which is confirmed that it depends on the HI and HSN.

Keywords: Pool boiling, Transient boiling, Critical heat flux, Exponential heat generation rate

1. Introduction

It is important to understand the mechanism and corresponding correlation for the boiling heat transfer for the effective use of existing energy conversion technology, so we need to accumulate the fundamental database of critical heat fluxes (CHFs) on energy conversion. Besides, the detailed understanding for generalized saturated and subcooled pool boiling CHF mechanisms and those correlations in non-wetting and wetting liquids, for wide range of subcoolings and pressures due to steady and transient heat inputs is becoming increasingly important not only for the academic knowledge on the complex transition phenomena but also for the fundamental database of following problems: the transient thermal response of reactivity accident and the engineering safety evaluation of a nuclear reactor, the design such as the high heat flux cooling systems using subcooled water pool boiling, the super-conducting magnets cooled by liquid helium and liquid nitrogen, the thermal control of microelectronic assemblies cooled by FC liquids for future super-computers and so on. Furthermore, the evaluation of the pool boiling CHF becomes the database for the derivation of subcooled flow boiling CHF correlations based on the pool boiling ones, and it is also an essential problem when the liquid flow in the cooling equipment stops due to accidents.

Many aspects of saturated and subcooled pool boiling CHF have been investigated by many researchers for pressures, subcoolings, test heater configurations, surface conditions, thermal properties, etc., assuming a CHF model mainly based on a kind of hydrodynamic instability (HI) at CHF. Recently the saturated and subcooled pool boiling CHF for

* 商船学科 ** 神戸大学 2006 年 9 月 29 日受付

a horizontal cylinder in water and wetting liquids were measured for comparatively wide range of pressures and subcoolings. Then it was presented that there exists a new physical model due to explosive-like heterogeneous spontaneous nucleation (HSN) on the cylinder surface. According to the new physical model, it is thought basically that HSN model significantly depends on the surface energy and the cavity size distribution from a physical model on CHF. This research is to clarify the mechanism of CHF which is confirmed that it depends on the HI and HSN model, and to apply a new physical model.

The typical trend of the CHF values in relation to the heat generation rates shown with period is as follows: the CHF gradually increases with the decrease in period up to the maximum CHF from the steady-state one corresponding to the CHF for the period of 20 s, then the CHF decreases down to the minimum one and again increases with the decrease in period. It is assumed that there exist two different CHF mechanisms related to the period. The measured CHFs related to subcoolings for water, liquid nitrogen and liquid helium with pressures as a parameter disagreed with the corresponding values derived from the existing correlations given by Kutateladze [1] and Zuber [2] based on the model of CHF resulting from hydrodynamic instability (HI). However, those data were well described by the newly derived subcooled pool boiling CHF correlations derived by Fukuda et al. [3] and Sakurai et al. [4]-[8] by assuming that CHFs occur due to the hydrodynamic instability (HI), or the heterogeneous spontaneous nucleation (HSN) in originally flooded cavities which coexists with vapor bubbles growing up from active cavities.

Recently Chang et al. [9] measured CHF and corresponding surface superheat at which the transition from natural convection regime to film boiling in a pool of FC-87, and also measured minimum film boiling heat flux and corresponding surface superheat. They confirmed that both surface superheats at the transition point from natural convection region to film boiling, and the collapse point of minimum film boiling caused by steadily increasing and decreasing heat inputs respectively, agreed with each other. They concluded that the film boiling incipience at the transition point and minimum film boiling at collapse point occur due to the lower limit of HSN in wetting liquid of FC-72 and FC-87 based on the theory of Sakurai et al. [7],[8]. Takahashi et al. [10] has measured the dynamic heat transfer processes due to an exponential heat input for a 1.2 mm diameter horizontal cylinder in a pool of FC-72 at the pressures of 101.3 kPa and 150 kPa. They have assumed that the mechanism of the direct transition from non-boiling regime to film boiling regime is a consequence of the HSN.

In the present work, the boiling phenomena and critical heat fluxes were experimentally investigated using a horizontal cylinder in a pool of ethanol for wide range of subcoolings and pressures caused by the exponential heat generation rates with the e-fold times, period. Also, it is clarified that the trend of CHF values explained by the HI and/or HSN significantly depends on experimental conditions such as the pressure, subcooling and period.

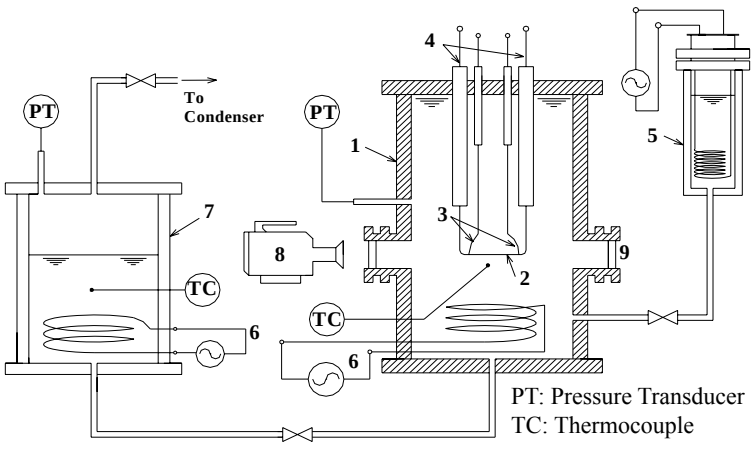

Fig. 1 Schematic diagram of experimental apparatus.

2. Experimental apparatus and method

Figure 1 shows the schematic diagram of experiment apparatus which consists of a boiling vessel and a test heater inside the vessel, pressurizer, subcooling and heat generation rate controlling system, measurement and data processing system and a high-speed video camera.

The boiling vessel with inspection windows is made of stainless steel having an inner diameter of 200 mm and a height of 600 mm. The test heater is made of platinum wire having a diameter of 1.0 mm, which is horizontally mounted in the vessel. The cylinder diameter is from the reference paper reported by J. H. Lienhard et al. [11],[12] showing with the prediction curve for cylinder. The effective length of heater between the potential taps is about 31 mm. The heater was annealed in order to maintain an even properties and its electrical resistance versus temperature relation was calibrated in water and glycerin baths using a precision double bridge circuit. The calibration accuracy was estimated to be within ±0.5 K.

The average temperature of the test heater was measured by resistance thermometry using the heater itself. A double bridge circuit with the heater as a branch was first balanced at the bulk liquid temperature. The output voltages of the bridge circuit, together with the voltage drops across the potential taps of the heater and across a standard resistance, were amplified and passed through analog-to-digital (A/D) converters installed in computer. These voltages were simultaneously sampled at a constant time interval that was changed depending on period. The fastest sampling speed of the A/D converter was 5 μs/channel. The average temperature was obtained by using the previously calibrated resistance-temperature relation. The heat generation rate of the test heater was determined from the current to the heater and the voltage difference between potential taps on the test heater. The surface temperature was obtained by solving the conduction equation in the heater under the conditions of the average temperature and heat generation rate. The instantaneous surface heat flux was obtained from the heat balance equation for a given heat generation rate. The experimental error was estimated to be about ±1 K in the heater surface temperature and ±2 % in the heat flux.

The electric current was supplied to the test heater directly with a constant voltage direct-current power supply (maximum current 700A) which provides a heat generation rate increased by exponential function, $Q = Q_0 \exp^{t/\tau}$. It was given exactly regardless of resistance changes of heater due to temperature change of heater. A high speed video camera system (1000 frames/s with a rotary shutter exposure of 1/10000 s) is used to observe the boiling phenomena and to confirm the start of boiling on the test heater surface.

The test liquid was degassed by keeping boiling and evacuating vapor for 30 minutes at least in the liquid feed tank. The test liquid was fully filled in the boiling vessel with the free surface only in the pressurizer and liquid feed tank. Liquid temperatures in the boiling vessel and in the pressurizer were separately controlled to realize the desired saturated and subcooled conditions. Table 1 shows the experimental conditions.

Table 1. Experimental conditions.

Test heater	platinum wire
Test liquid	ethanol
Pressures	101.3 - 1572 kPa
Subcoolings	0 - 160 K
Periods	5 ms - 50 s

3. Typical trend of CHF versus period

Fukuda et al. [3] suggested the several empirical equations representing transient CHF values versus periods belonging to the first and second groups in a pool of water for wide ranges of subcooling and pressure. The CHF belonging to the first group caused by the heat generation rates with a long period under a lower subcooling condition

and a higher subcooled one is expressed by the Eq. (1) and Eq. (2), respectively. The CHF belonging to the second group with a short period is expressed by the Eq. (3).

$$q_{cr} = q_{st,sub}\left(1+0.21\tau^{-0.5}\right),\ \text{1st group for lower subcooling} \tag{1}$$

$$q_{cr} = q_{st,sub}\left(1+2.3\times10^{-2}\tau^{-0.7}\right),\ \text{1st group for higher subcooling} \tag{2}$$

where the $q_{st,sub}$ is given by the quasi-steady-state CHF data in each experiment.

$$q_{cr} = h_c\left(\Delta T_{in}(\tau)+\Delta T_{sub}\right),\ \text{2nd group} \tag{3}$$

where $h_c = (k_l\rho_l c_{pl}/\tau)^{1/2}K_{1th}(\mu D/2)/K_0(\mu D/2) \cong (k_l\rho_l c_{pl}/\tau)^{1/2}$, and $\mu = [\rho_l c_{pl}/k_l\tau]^{1/2}$. K_o and K_{1th} are the modified Bessel functions of the second kind of zero- and first-orders. The symbol of h_c is the heat transfer coefficient resulting from transient heat conduction, $\Delta T_{in}(\tau)$ is the initial boiling surface superheat due to the HSN in conduction regime, and ΔT_{sub} is liquid subcooling.

The trend of q_{cr} expressed by the Eq. (1) is due to the hydrodynamic instability (HI) at which the transition from fully-developed nucleate boiling (FDNB) to film boiling occurs. The transition mechanism has been already pointed out by Kutateladze [1] and Zuber [2]. The trend that the q_{cr} values gradually increases with a decrease in period for the group is explained by the time lag of the HI by which the transition to film boiling occurs at the steady-state q_{cr} (Sakurai et al. [6]). On the other hand, the steady-state CHF, $q_{st,sub}$, values for the subcooling higher than around 60 K at the higher pressures except the pressures lower than around 300 kPa become lower than those expected by the correlation based on the HI. It was assumed by Sakurai et al. [7] that the transition to film boiling at the steady-state CHF, $q_{st,sub}$, due to the heat generation rate with the long period such as 20 s for subcoolings higher than around 60 K at pressures higher than around 400 kPa occurs due to the HSN at a lower limit of HSN temperature. Therefore, the trend of q_{cr} values related to periods, expressed by the Eq. (2), become different from the corresponding curve estimated by Eq. (1) due to the HI. The q_{cr} data in relation to the periods also gradually increases with a decrease in period because the HSN surface superheat depends on an increasing rate of surface superheat as mentioned previously by Sakurai et al [6].

The second group of q_{cr} for the periods shorter than the period corresponding the minimum q_{cr} is expressed by the Eq. (3). The q_{cr} values for the periods at each pressure are expressed by a linear asymptotic line on a log-log graph, and those are considered that the direct boiling transition on the heater surface from non-boiling to film boiling is based on the HSN as mentioned before. As shown in the subsequent experimental results, the empirical equations (1)-(3) are also effective for the highly wetting liquids such as ethanol.

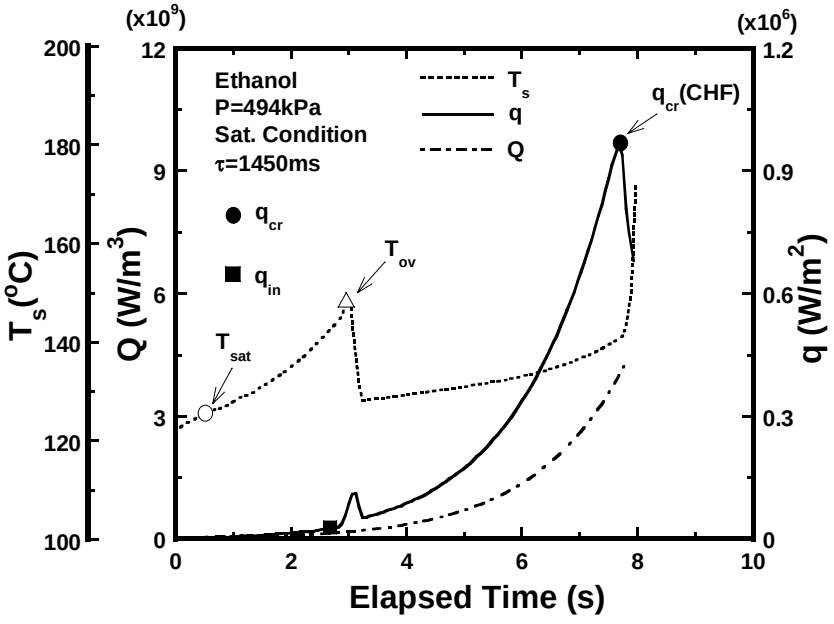

Fig. 2 Illustrative time traces of heat input, Q, heater surface temperature, T_s and heat flux, q.

4. Experimental results and discussion

4.1. Transient heat transfer process under saturated condition

Figure 2 shows typical changes in the heater surface temperature, T_s, and heat flux, q, with time for an exponential heat input, Q, with a period of 1450 ms at a pressure of 494 kPa under saturated conditions. As shown in the figure, the surface temperature of heater increases with an increase in heat input. Incipient boiling starts at a point where corresponds to the q_{in} beyond saturation temperature, T_{sat}. The heater temperature continues to increase up to T_{ov}, then decreases and again increases with an increase in heat input. Since the heat flux reaches the critical heat flux point, q_{cr}, the heater surface temperature rapidly increases with time.

4.2. Transient boiling process with transition to film boiling under saturated condition

Figure 3 shows the transient phenomenon on a graph of heat flux, q, versus surface superheat, ΔT_{sat}, for the same conditions in Fig.2. The surface superheat ΔT_{sat} is defined by the difference between the surface temperature of the heater and the saturation temperature corresponding to the system pressure. The steady-state natural convection curve derived by Takeuchi et al. [13] and the steady-state film boiling curve derived by Sakurai et al. [14], are also shown in the figure for comparison.

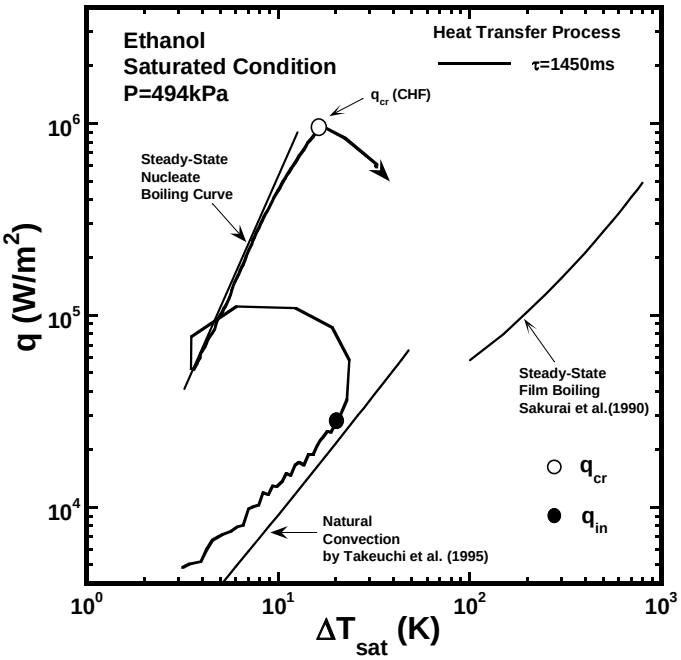

Fig. 3 Boiling heat transfer processes from non-boiling to fully developed nucleate boiling for the same conditions in Fig.2.

The boiling process caused by a steadily increasing heat input with a period of 1450 ms is as follows: heat flux, q, increases along slightly above the natural convection curve at first and after the occurrence of initial boiling, the surface superheat rapidly decreases, and q increases along the steady-state nucleate boiling curve and reaches the CHF point, q_{cr}, near the extension of the curve and then the transition to film boiling occurs. The rising curve of non-boiling regime up to the initial boiling, q_{in}, lies on the left hand side of the steady-state natural convection curve. It means the effect of heat conduction exists. This is described in the next paragraph.

4.3. Heat transfer under non-boiling regime

Figure 4 shows typical experimental results of the heat transfer coefficient, h, before the initiation of boiling for ethanol as a function of period, τ. For a reference, the transient heat conduction correlation (h_c), the steady-state natural convection heat transfer correlation (h_n), and the combined heat transfer correlation (h_m) were also shown in the figure. As shown in the figure, heat transfer processes from the heater surface when the heat generation rate increased with exponential function under non-boiling state are as follows; as the period shortens, heat transfer due to the heat conduction becomes predominant from natural convection heat transfer, and in the region of the period over a second (τ> 1 s), the heat transfer is considered to be quasi-steady-state heat transfer. In this study, heat transfer processes for the

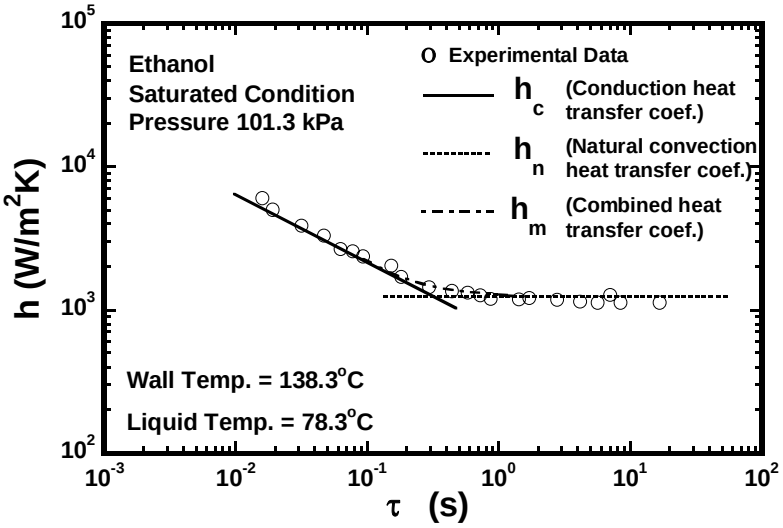

Fig. 4 Heat transfer coefficient before the initiation of boiling as a function of exponential period.

periods longer than 10 s are considered as quasi-steady-state one because the non-boiling region agreed with natural convection heat transfer, and all CHFs measured for the heat inputs with periods longer than 10 s are almost the same.

4.4 Heat transfer processes during transitions to fully-developed nucleate boiling or to film boiling at a pressure of 101.3 kPa in saturated ethanol

Figure 5 shows the heat transfer processes in saturated ethanol on a graph of heat flux, q, versus surface superheat, ΔT_{sat}, for the periods of 50 s and 100 ms at atmospheric pressure. The steady-state natural convection curve [13], the steady-state film boiling curve [14] and heat conduction curve [15] are shown in the figure for comparison. The processes from non-boiling to film boiling are completely different from each other depending on the periods. The heat transfer process for a period of 50 s is shown with a solid line where photographs were taken at the points of 7(a) to (f). On the other hand, the process for a period of 100 ms is shown with a dashed line where photographs were taken at the points of 6(a) to (f): the boiling process shows that the q value increases along the heat transfer curve of heat conduction, then shows a transition directly to film boiling without passing the nucleate boiling. The boiling occurs at a surface superheat point of 100 K, which is higher than that in the case of the process at period of 50 s. It could be seen that the initial boiling surface superheat at which direct transition occurs, became a little higher with a decrease in period. Also, the initial boiling temperature gradually decreased with an increase in system pressure based on experimental data. It is considered that the direct boiling transition on the heater surface from non-boiling to film boiling is due to the heterogeneous spontaneous nucleation (HSN) in previously flooded cavities on heater surface as suggested by Sakurai et al. [4]-[8].

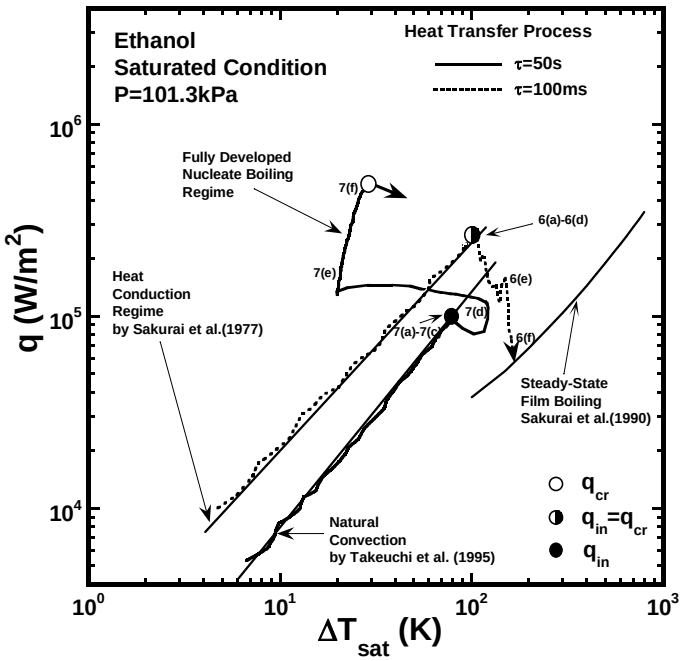

Fig. 5 Boiling heat transfer process from non-boiling to film boiling or to fully developed nucleate boiling in ethanol Photographs were shown in Figs. 6 & 7.

Then the Figs 6 and 7 give a series of subsequent photographs at the same condition in Fig.5. In the case of a period of 100ms at first, the photo no. 6(b) taken at 2 ms after the first one shows a vapor tube due to the explosive boiling in flooded cavities, the vapor bubbles are rapidly growing and covering the heater surface within just a few milliseconds,

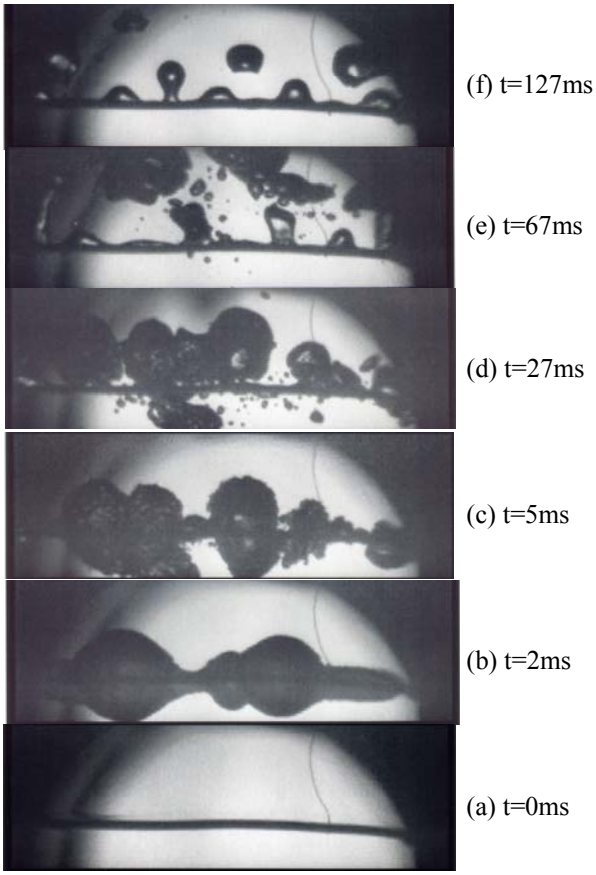

Fig. 6 Vapor film behavior during direct transition to film boiling for a period of 100 ms at a pressure of 101.3kPa in saturated ethanol.

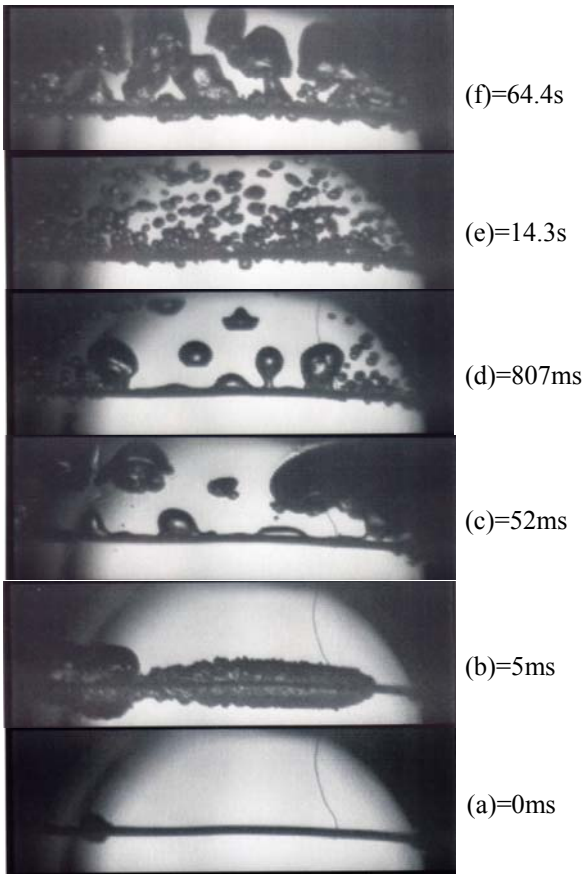

Fig. 7 Vapor film behavior during transition to fully developed nucleate boiling for a period of 50 s at a pressure of 101.3kPa in saturated ethanol.

and it shows the vapor bubbles collapse from the boiling initiation bubbles as shown in 6(c). Then, large vapor bubbles are broken away from the large vapor film by buoyancy force and move upward like 6(d). Here is around the CHF. After detachment of the large vapor bubbles, solid-liquid contacts occurs, and then new thin vapor film with the Taylor unstable wave on the upper part of the vapor-liquid interface covering the cylinder is formed by the explosive-like HSN on the places of solid-liquid contact and thin film boiling. At this moment the surface temperature starts increasing rapidly as a result of heat transfer deterioration. As shown in figure 6(f), the behavior of vapor-liquid interface in film boiling on the cylinder similar to that for steady-state film boiling on the cylinder is clearly observed after the detachment of large vapor bubbles.

On the other hand, in the case of a period of 50 s, Fig. 7(a) is the onset of boiling on the heater. The photo no. 7(b) taken at 5 ms after the first one shows that it covers the whole heater surface by the large vapor tube. The occurrence behavior of initial boiling is just similar to that of the direct transition for 100 ms. This vapor film behavior that is rapidly growing and covering the heater surface during boiling initiation is the strong point of this kind of liquid. Highly wetting liquids such as ethanol is that the surface tension is lower than that of water and its contact angle between liquid and heater surface is also smaller than that of water, so that it may be easy for a wetting liquid to previously flooded cavities on a heater surface. Therefore, it can be assumed that the initial boiling is due to flooded cavities on a heater surface. After the detachment of large vapor bubbles, transition to fully-developed nucleate boiling occurs.

4.5 Steady-state critical heat flux (steady CHF) under subcooled condition

In this experiments, heat transfer processes for the periods longer than 10 s are considered as quasi-steady- state ones as mention before. Figure 8 shows steady-state CHF data related to subcoolings with pressure as a parameter in a pool of ethanol with corresponding CHF curves obtained by empirical equations, Eqs. (4) and (5) for comparison. As shown in the figure, the CHFs dependent on pressure exist in a very narrow range of low subcoolings near saturated condition, and they gradually increase with an increase in subcooling. The CHF values for higher subcoolings are independent of pressure.

As mentioned before, Sakurai et al. [7] has reported that CHF data obtained for high subcoolings at high pressures in a pool of water are due to the HSN. The mechanism of heat transfer crisis at CHF and the properties, i.e., latent heat of vaporization, surface tension, density of saturation liquid etc. are greatly affected in CHF correlation. In the case of CHF data in a pool of ethanol which is highly wetting liquid, it has lower surface tension and its contact angle on heater surface is smaller than that of water, so that it may be easy for a wetting liquid such as ethanol to flood cavities on a heater surface. Therefore, it can be assumed that the CHF belonging to second group for lower subcooling is due to HSN.

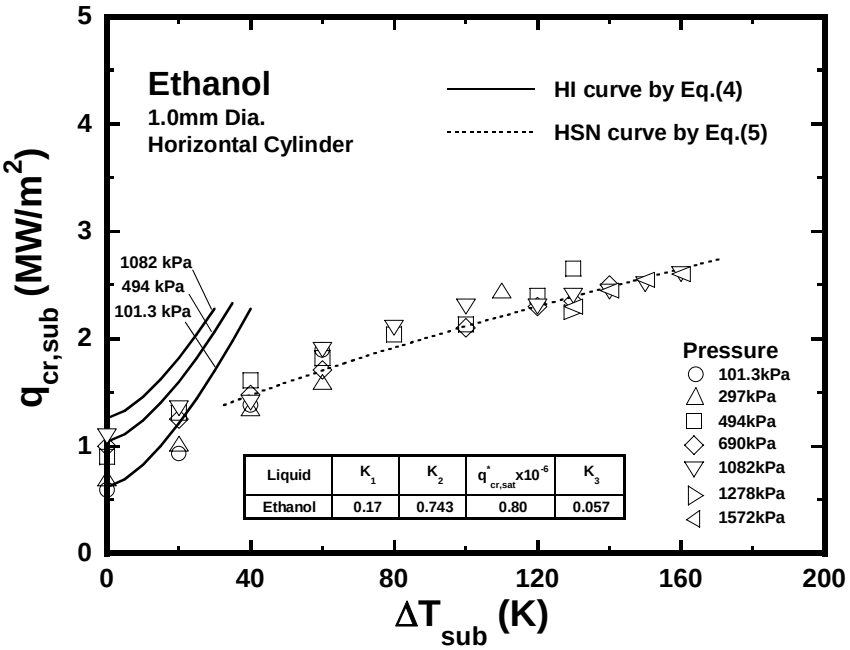

Fig. 8 Comparison of prediction representing $q_{cr,sub}$ related to subcooling at pressure as a parameter in ethanol using Eq. (4) and (5).

$$q_{cr,sub} = q_{cr,sat}\left[1 + K_2\left(\rho_l/\rho_v\right)^{0.69}\left(C_{pl}\Delta T_{sub}/L\right)^{1.5}\right] \quad (4)$$

where, $q_{cr,sat} = K_1 L\rho_v\left[\sigma g(\rho_l - \rho_v)/\rho_v^2\right]^{0.25}$

$$q_{cr,sub} = q^*_{cr,sat}\left(1 + K_3\Delta T_{sub}{}^{0.73}\right) \quad (5)$$

$q^*_{cr,sat}$ resulting from the HSN for zero subcooling.

The obtained K_1 and K_2 are 0.17 and 0.743 respectively. The values of $q^*_{cr,sat}$ and K_3 are 0.80×10^6 and 0.057 respectively as shown in the figure. The measured $q_{cr,sub}$ values lie almost within ±12% differences of the values obtained by Eq. (5) resulting from HSN.

4.6 Transient critical heat flux (transient CHF)

4.6.1 The q_{cr} for period under saturated condition

Figure 9 shows transient CHFs, q_{cr} versus the periods, τ, ranging from around 50 s down to 5 ms under saturated condition at various pressures in ethanol. As shown in the figure, the q_{cr} values for all periods gradually increase with a decrease in period up to the maximum CHF from the steady state one corresponding to the CHF for a period of 10 s or

more, and then decrease down to the minimum one and again increase with a decrease in period. Also the CHF values in relation to the periods can be divided into three principal groups as shown in the figure; the first groups are shown with a solid line, and the second groups are shown with a dashed line. The q_{cr} values for the periods belonging to the first group at the saturated pressures are well expressed by Eq. (1), also the q_{cr} values for short periods belonging to the second group for each pressure are approximately expressed by Eq. (3).

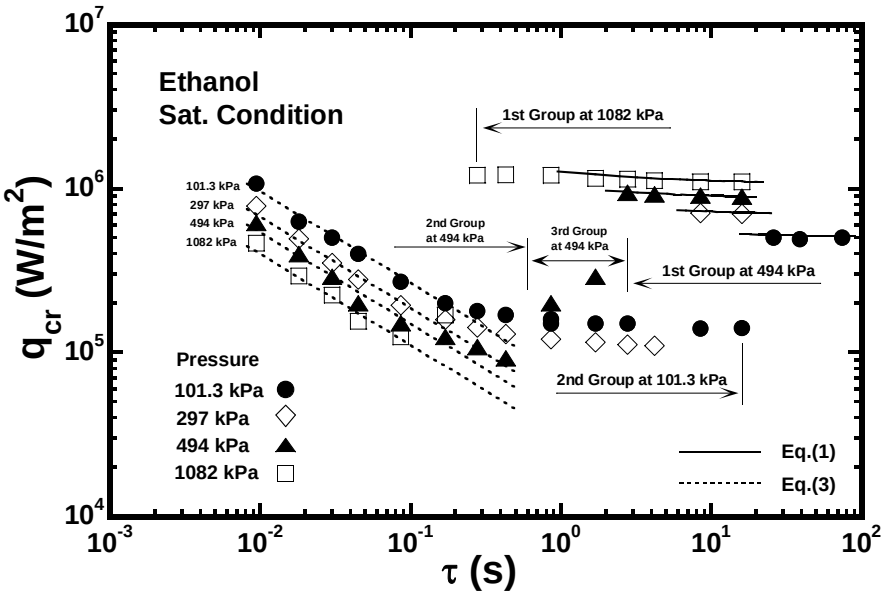

Fig. 9 The relation between q_{cr} and τ in at various pressures in saturated ethanol.

In the case of the saturated condition at various pressures, the q_{cr} values for periods belonging to the first group are well dependent on pressure. The increasing trend of q_{cr} is explained by the time lag of heat transfer crisis at steady-state critical heat flux, q_{st}. As for the second group shown with a dashed line at each pressure, the q_{cr} decreases with an increase in pressure with a constant period because the lower limit of HSN surface superheat decreases with an increase in pressure. As seen in the figure, the shortest period for the q_{cr} belonging to the third group becomes shorter with an increase in pressure. Therefore, the q_{cr} at the longest period which belongs to the second group could not be observed at higher pressures by the heat input with the shortest period tested here. The minimum q_{cr} for the period under the pressure of 494 kPa for the saturated condition is observed at around 0.4 s. It should be noted that the value is about 14% of steady-state one corresponding to the CHF for the period of 10 s. As a result from the experimental data, the minimum q_{cr} values within the second group at each pressure were much lower than the corresponding steady state CHF. This fact means that conduction heat transfer becomes more predominant as the period becomes shorter than natural convection heat transfer. Therefore, the heat transfer coefficient becomes higher due to heat conduction and a direct or semi-direct transition to film boiling occurs at the heat flux point that is higher than that of natural convection.

4.6.2 The q_{cr} for period under subcooled condition

The experimental data obtained for the pressure of 690 kPa for the subcoolings over range of 0 to 100 K in ethanol are shown in Fig. 10 versus exponential period as a typical. The curves representing the q_{cr} for τ for the subcooling of 0 K, namely the saturated condition, derived form Eq. (1) is shown in the figure with a solid line. The values of q_{cr} increase gradually with a decrease in period up to those at the periods around 2 s for the subcooling of 0 K. As mentioned before, the trend of q_{cr} for τ was explained as the time lag of heat transfer crisis which occurs at steady-state q_{cr}. On the other hand, the values of q_{cr} for periods for subcoolings higher than 20 K are expressed by the Eq. (2) with a dashed chain line, and those are lower than the values predicted by the Eq. (1). The values of q_{cr} for the liquid subcoolig of 100 K increase more gradually with a decrease in period up to those at the period around 0.4 s. The trend

of q_{cr} for period is explained due to the effect of increase in HSN surface superheat dependent on the increasing rate of surface superheat at the incipience of HSN.

The value of q_{cr} for the period of 10 s, namely steady-state critical heat flux, for subcooling of 0 K is a little bit lower than that described by Eq. (4) based on HI, so the $q_{st,sub}$ value measured in the experiment was used and expressed by Eq. (1). And the values for the subcoolings higher than 20 K are due to the HSN and described by Eq. (2) as mentioned in Section 4.5 and can be seen in Fig. 8. As for the second group shown with a dashed line at each subcooling, the q_{cr} increases with an increase in subcooling and well dependent on liquid subcooling. As seen in the figure also, the longest period for the q_{cr} belonging to the second group becomes shorter with an increase in subcooling. It can be assumed that the q_{cr} at the longest period which belongs to the second group won't be observed at higher subcoolings for the exponential heat input with the shortest period.

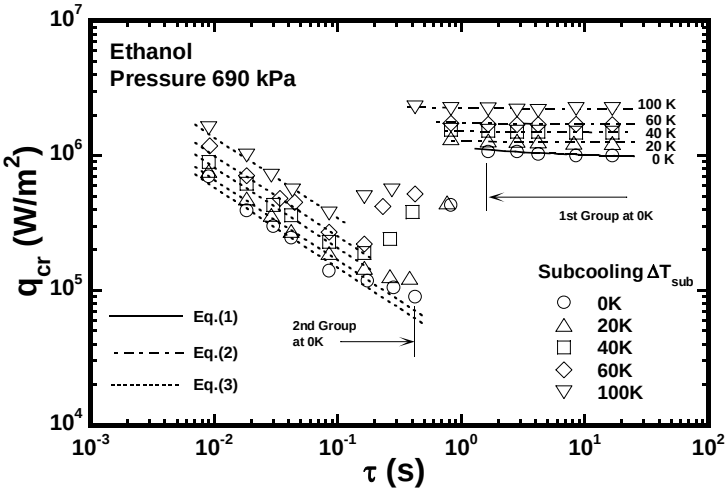

Fig. 10 The relation between q_{cr} and τ for various subcoolings at pressure of 690 kPa in ethanol.

Figure 11 shows transient CHFs, q_{cr} versus periods, τ, for the subcooling of 40K and 130 K at each pressure in ethanol. The q_{cr} values are clearly divided into three principal groups depending on the periods. The first group with a period longer than around 1 s is shown with a dashed chain line expressed by Eq. (2), and the second group with a period shorter than around 0.1 s is shown with a dashed line expressed by Eq. (3). As seen in the figure, q_{cr} values clearly increase with an increase in subcooling. However they are almost independent of pressure. The steady-state CHFs for high subcooling at the pressures are also independent of the pressures as shown in Fig.8. Sakurai et al. [6] have explained this fact by assuming that the transition to film boiling at the steady-state CHFs occurs due to the explosive-like HSN in FDNB regime. The minimum CHFs for the period of around 0.1 s are observed. The trend of q_{cr} for periods belonging to the first and second groups are well expressed because the CHFs at which the transitions to film boiling occur due to the HSN instead of the hydrodynamic instability as mentioned before.

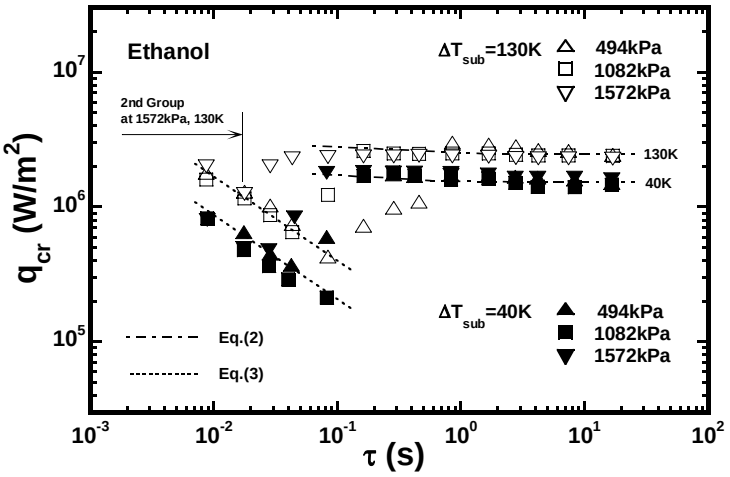

Fig. 11 The relation between q_{cr} and τ for various subcoolings and pressures in ethanol.

5. Conclusions

Steady-state and transient boiling heat transfer are experimentally investigated for exponential heat generation rates at various periods in a highly wetting liquid such as ethanol, and the following results are obtained.

(1) The quasi-steady-state CHFs measured were mainly divided into two mechanisms for lower and higher subcooling at pressure; the former and latter CHFs occurred due to hydrodynamic instability (HI) and explosive-like heterogeneous spontaneous nucleation (HSN) on the cylinder surface respectively. The CHFs were dependent on pressure in low subcoolings, and the CHF values for higher subcoolings were independent of pressure and gradually increase with an increase in subcooling.

(2) The transient CHFs were clearly classified into three principal groups for the periods: first group for the longer period, second group for the shorter and third group for the intermediate. And those were dependent on subcooling in the case of a constant pressure. The CHFs belonging to the first group for longer periods at lower and higher subcoolings at the pressure, expressed by Eq. (1) representing CHF due to the HI, and Eq. (2) representing CHF due to the HSN, respectively, were effective for a highly wetting liquid. Also, the second groups of CHFs for the shorter periods were approximately expressed by Eq. (3) which gave the theoretical conduction heat flux corresponding to a short period at the corresponding HSN surface superheat depending on the period.

(3) The minimum CHF values for the longest period for the second group were much lower than the corresponding steady-state CHF. The shortest period for the q_{cr} belonging to the third group became shorter with an increase in pressure and subcooling. It can be assumed that the q_{cr} at the longest period belonging to the second group won't be observed at higher pressures and subcoolings by the heat generation rate with shortest period. Consequently, the CHF values belonging to the second and third group were considerably affected by the heat generation rates shown with period.

Nomenclature

c_p Specific heat at constant pressure, J/(kgK)

D Cylinder diameter, m

h_{lv} Latent heat of vaporization, J/kg

K_1 Coefficient in Eq. (3)

k Thermal conductivity, W/(mK)

p Pressure, Pa

p_c Critical pressure, Pa

Q Heat generation rate, W/m^3

Q_o Initial heat generation rate, W/m^3

q_{cr} Critical heat flux, W/m^2

$q_{cr,sat}$ q_{cr} for saturated condition, W/m^2

q_{st} Steady-state critical heat flux, W/m^2

q_{in} Boiling initiation heat flux, W/m^2

T_w Heater surface temperature, K

$\Delta T_{sat} = (T_w - T_{sat})$, Surface superheat, K

$\Delta T_{sub} = (T_{sat} - T_B)$, Liquid subcooling, K

Abbreviations

CHF Critical heat flux

FDNB Fully-developed nucleate boiling

T_{sat} Saturated temperature, K

T_B Bulk liquid temperature, K

t Time, s

Greek symbols

ρ Density, kg/ m^3

σ Surface tension, N/m

τ Period, s

Subscript

l Liquid

v Vapor

HI　Hydrodynamic instability

HSN　Heterogeneous spontaneous nucleation

Period　The e-fold time corresponding to heat generation rate with the exponential increasing rates from quasi-steady to rapid ones.

References

[1] Kutateladze, S.S., "Heat transfer in condensation and boiling," AEC-tr-3770, USAEC (1959).

[2] Zuber, N., "Hydrodynamic Aspects of Boiling Heat Transfer," AECU-4439, USAEC (1959).

[3] Fukuda, K., Shiotsu, M. & Sakurai, A., "Transient pool boiling heat transfer due to increasing heat inputs in subcooled water at high pressures," Proceedings of the 7th Int. Meeting on Nuclear Reactor Thermal Hydraulics, Saratoga Springs, USA (1995), pp. 554-573.

[4] Sakurai, A., Shiotsu, M. & Hata, K., "New transition phenomena to film boiling due to increasing heat inputs on a solid surface in pressurized liquids, Instability in Two Phase Flow Systems," Vol. HTD-260/Fed-169. ASME, New York (1993), pp. 27-39.

[5] Sakurai, A., Shiotsu, M. & Hata, K., "Mechanism of nucleate boiling on a solid surface in liquid helium," Advances in Cryogenic Engineering, 39A (1994), pp. 1759-1768.

[6] Sakurai, A., Shiotsu, M., Hata, K. & Fukuda, K., "Transition phenomena from non-boiling regime to film boiling on a cylinder surface in highly subcooled and pressurized water due to increasing heat inputs," ASME Paper, 95-WA/HT-17 (1995), pp.1-11.

[7] Sakurai, A., Shiotsu, M. & Fukuda, K., "Pool boiling critical heat flux on a horizontal cylinder in subcooled water for wide ranges of subcooling and pressure and its mechanism," Proceedings of the Thirty-first National Heat Transfer Conference, Vol. HTD-326, ASME, New York (1996), pp. 93-104.

[8] Sakurai, A., "Mechanisms of transitions to film boiling at CHFs in subcooled and pressurized liquids due to steady and increasing heat inputs." *Nuclear Engineering and Design*, Vol. 197 (2000), pp. 301-356.

[9] Chang, J.Y., You, S.M. & Haji-Sheikh, A., Film boiling incipience at the departure from natural convection on flat, smooth surfaces, ASME *Journal of Heat Transfer*, Vol. 120 (1998), pp. 402-409.

[10] Kasakawa, Takashi, K., Hata, K. & Shiotsu, M., Transient heat transfer on a horizontal cylinder in FC-72, Advances in Electronic Packaging 1999, ASME EEP Vol. 26-2 (1999), pp. 1471-1478.

[11] J. H. Lienhard, "Burnout on Cylinders" *Journal of Heat Transfer*, Vol. 110 (1988), pp.1271-1286.

[12] J. H. Lienhard & V. K. Dhir "Hydrodynamic Prediction of Peak Pool-boiling Heat Fluxes from Finite Bodies" *Journal of Heat Transfer*, Vol. 95, No. 2 (1973), pp.1271-1286.

[13] Takeuchi, Y., Hata, K., Shiotsu, M. & Sakurai, A., A general correlation for laminar natural convection heat transfer from single horizontal cylinders in liquids and gases with all possible Prandtl numbers, International Mechanical Engineering Congress and Exposition, Vol. HTD-317-1. ASME, New York (1995), pp. 259-270.

[14] Sakurai, A., Shiotsu, M. & Hata, K., A general correlation for pool film boiling heat transfer from a horizontal cylinder to subcooled liquid, Part 2: experimental data for various liquids and its correlation. ASME *J. Heat Transfer*, Vol. 112 (1990), pp.441-450.

[15] Sakurai, A. & Shiotsu, M., "Transient pool boiling heat transfer, Part 1: incipient boiling superheat." ASME *J. Heat Transfer*, Vol. 99 (1977), pp. 547-553.